

Size effects of solvent molecules on the phase behavior and effective interaction of colloidal systems with the bridging attraction

This content has been downloaded from IOPscience. Please scroll down to see the full text.

2016 J. Phys.: Condens. Matter 28 455102

(<http://iopscience.iop.org/0953-8984/28/45/455102>)

View [the table of contents for this issue](#), or go to the [journal homepage](#) for more

Download details:

IP Address: 129.6.121.180

This content was downloaded on 13/09/2016 at 13:58

Please note that [terms and conditions apply](#).

You may also be interested in:

[Settled and unsettled issues in particle settling](#)

Roberto Piazza

[The role of long-range forces in the phase behavior of colloids and proteins](#)

M. G. Noro, N. Kern and D. Frenkel

[Fluid–fluid demixing transitions in colloid–polyelectrolyte star mixtures](#)

Martin Konieczny and Christos N Likos

[Colloidal gels: equilibrium and non-equilibrium routes](#)

Emanuela Zaccarelli

[The physics of a model colloid–polymer mixture](#)

W C K Poon

[Depletion effects in binary hard-sphere fluids](#)

Thierry Biben, Peter Bladon and Daan Frenkel

[Gelation as arrested phase separation in short-ranged attractive colloid–polymer mixtures](#)

Emanuela Zaccarelli, Peter J Lu, Fabio Ciulla et al.

Size effects of solvent molecules on the phase behavior and effective interaction of colloidal systems with the bridging attraction

Jie Chen^{1,2}, Xuewu Wang¹, Steven R Kline² and Yun Liu^{2,3}

¹ Department of Engineering Physics, Tsinghua University, Beijing, People's Republic of China

² NIST Center for Neutron Research, Gaithersburg, MD 20899, USA

³ Department of Chemical and Biomolecular Engineering, University of Delaware, Newark, DE 19716, USA

E-mail: yunliu@nist.gov or yunliu@udel.edu

Received 12 April 2016, revised 22 July 2016

Accepted for publication 9 August 2016

Published 12 September 2016



Abstract

There has been much recent research interest towards understanding the phase behavior of colloidal systems interacting with a bridging attraction, where the small solvent particles and large solute colloidal particles can be reversibly associated with each other. These systems show interesting phase behavior compared to the more widely studied depletion attraction systems. Here, we use Baxter's two-component sticky hard sphere model with a Percus–Yevick closure to solve the Ornstein–Zernike equation and study the size effect on colloidal systems with bridging attractions. The spinodal decomposition regions, percolation transition boundaries and binodal regions are systematically investigated as a function of the relative size of the small solvent and large solute particles as well as the attraction strength between the small and large particles. In the phase space determined by the concentrations of small and large particles, the spinodal and binodal regions form isolated islands. The locations and shapes of the spinodal and binodal regions sensitively depend on the relative size of the small and large particles and the attraction strength between them. The percolation region shrinks by decreasing the size ratio, while the binodal region slightly expands with the decrease of the size ratio. Our results are very important in understanding the phase behavior for a bridging attraction colloidal system, a model system that provides insight into oppositely charged colloidal systems, protein phase behavior, and colloidal gelation mechanisms.

Keywords: bridging attraction, sticky hard sphere, size effect

 Online supplementary data available from stacks.iop.org/JPhysCM/28/455102/mmedia

(Some figures may appear in colour only in the online journal)

1. Introduction

Colloidal systems exist in various products in our daily life, such as shampoo, detergent, paint, food, microemulsions [1], therapeutic drugs [2], and biological systems [3–5]. One of the widely studied model systems is the depletion attraction system where there is no attraction between the added small

polymers (or small colloidal particles) and the large solute colloidal particles [6–20]. Due to the osmotic pressure, the small solvent particles can introduce an effective attraction between large colloidal particles. Depletion attraction systems with spherical particles have been widely used as model systems to study many of the fundamental problems in complex colloidal systems, such as gelation and glass transition [6, 14].

However, there are also a wide range of colloidal systems in which small solvent particles (or polymers) can be reversibly associated with large colloidal particles. When the attraction between small and large colloidal particles is strong enough, small particles can serve as bridges to connect neighbouring particles. This type of bridging attraction is common in many colloidal systems, such as oppositely charged colloidal systems [21, 22] and concentrated protein solutions with counterions [23, 24]. Much less attention has been paid to study model colloidal systems with bridging attractions.

Recently, a system consisting of poly N-isopropylacrylamide (PNIPAM) and polystyrene (PS) has been studied [25–27] in which the size ratio of small PNIPAM particles to large PS particles is about 0.14. It was found that there is an attraction between PNIPAM and PS particles [25], resulting in a bridging attraction. In these experiments [25, 26], the addition of small PNIPAM particles drive the system through a liquid–gel–liquid–gel phase transition. By assuming that both PNIPAM and PS particles can be approximated as spherical particles [28], we have recently calculated the theoretical equilibrium phase diagram for this system using Baxter’s multi-component sticky hard sphere (SHS) model [29, 30]. The spinodal decomposition regions, percolation transitions, and binodal regions are calculated using the parameters reported in the experimental data, and show good agreement with most experimental observations [28].

One of the most interesting features of bridging attraction systems is that the spinodal and binodal regions can form isolated islands in the phase space of small particle and large particle concentrations [28]. Therefore, by controlling the particle size ratio and the attraction strength between small and large particles, the phase diagrams can be finely tuned. While it is sometimes difficult to alter the surface chemistry that determines the attraction between the small and large particles, the particle size is, in general, easier to control. Hence, we may control the phase behavior of a system by simply changing the particle size ratio. Therefore, it is very useful to understand how the relative size ratio affects the equilibrium phase diagrams of bridging attraction systems. In addition, it is known that different types of counterions sometimes have different effects on protein solution structures and phase diagrams [2, 23, 31, 32]. The detailed reasons for many of these observations are still under investigation. However, the bridging attraction is believed to play an important role in some cases [24, 28]. Since the size ratio between counterions and proteins can vary for different systems, the investigation of the size ratio effects is hence important to understand the protein behavior in concentrated solutions.

In this paper, we systematically study the phase behavior of bridging attraction systems for a very wide range of the size ratio and attraction strength between small and large particles with a focus on the size ratio effect. Using Baxter’s multi-component model, we find that the equilibrium phase diagram of a bridging attraction system is very sensitive to the size ratio and the attraction strength. These results significantly expand the parameter space investigated by a previous paper, which focused mainly on the comparison of the theoretical

calculations and experimental observations of one model system [28]. And our results thus provide important physical insights to help guide the design of future experimental systems and understand the complex phase behaviors of systems with different particle size ratio and attraction strength.

2. Sticky hard sphere model

The analytical solution of the inter-particle structure factor, $S(Q)$, of a SHS system was first provided by Baxter, by solving the Ornstein–Zernike (OZ) equations with Percus–Yevick (PY) closure [29, 33]. He also extended the solution to the multi-component case later [34] using the ‘Q method’ [30]. For a SHS system, the interaction between hard spheres is modeled as an attraction of an infinitesimal range with an infinitely strong attraction strength. The pair potential of a multi-component SHS system between components i and j is expressed as:

$$\beta U_{ij} = \begin{cases} \infty, & r < \sigma_{ij}; \\ \ln[12\tau_{ij} \frac{d_{ij} - \sigma_{ij}}{d_{ij}}], & \sigma_{ij} < r < d_{ij}; \\ 0, & d_{ij} < r. \end{cases} \quad (1)$$

Here, $\beta = 1/(k_B T)$, k_B is the Boltzmann constant, and T is the absolute temperature. σ_i is the diameter of component i , $\sigma_{ij} = (\sigma_i + \sigma_j)$, and $d_{ij} - \sigma_{ij}$ is the attraction range between the component i and j . The sticky limit is achieved for $d_{ij} \rightarrow \sigma_{ij}$, where the attraction strength is infinitely large. And hereafter, we will use d_i for the diameter. τ_{ij} is the stickiness parameter that directly reflects the attraction strength, and can be considered as an effective temperature. When τ_{ij} is large, the attraction is weak while for small τ_{ij} , the attraction is strong. For a one-component SHS system, $\tau_1 = \tau$. In this case, there is a simple relationship between τ and the reduced second virial coefficient as $B_2^* = 1 - 1/(4\tau)$ [35]. The procedures and equations to solve the OZ equations for multi-component SHS systems have been given in details in the literature [28, 36–38]. A key step is to solve $N(N + 1)/2$ quadratic equations where N is the number of components. The solution is non-trivial for a two-component system for a general case.

However, for bridging attraction systems, the analytical solution of the OZ equation can be easily obtained. In a bridging attraction dominated system [28], there are two components. One is the large solute colloid particle, the other is the small solvent particle. There is no attraction between the like components, which means $\tau_{SS} = \infty$, $\tau_{LL} = \infty$. (The subscripts ‘S’ and ‘L’ represent small solvent particles and large solute particles respectively.) The only stickiness parameter with nonzero attraction is τ_{SL} and will simply be expressed as τ hereafter. This simplifies tremendously the work to solve the OZ equation. As a result, it is now very straightforward to obtain analytical solutions with the PY closure [28]. For this special case, the set of quadratic equations reduces to only one linear equation and analytical solutions exist for all the parameters [28], which provides the basis for theoretical analysis. The size ratio of the small to large particle is defined as $x = d_S/d_L$.

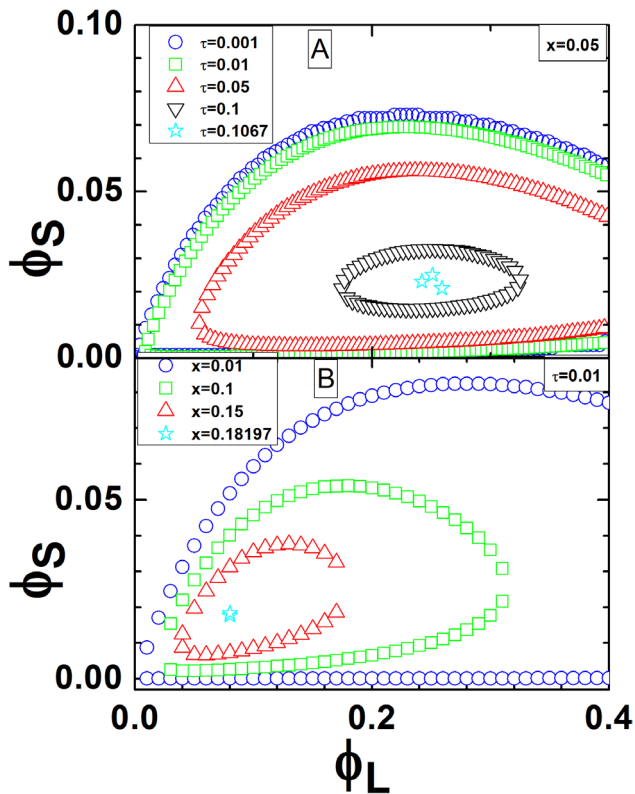


Figure 1. Spinodal decomposition island in the volume fraction plane for (A) different stickiness parameters with fixed size ratio $x = 0.05$ and (B) different size ratios with fixed stickiness parameter $\tau = 0.01$.

3. Results and disucssions

Using previously developed methods [28, 30], we have thus systematically explored the effect of the size ratio, x , and the stickiness parameter, τ , on the phase diagrams of bridging attraction systems. The spinodal regions are directly studied with Baxter’s two-component SHS theory. Therefore, the results are valid for all the size ratios, x . Hence the results are applicable not only for small x , but also for the cases where small particles have a comparable size with the large particles and cannot be considered as solvent molecules anymore. For the percolation transitions and binodal regions, we have focused on small x , where small particles can be treated as solvent molecules. For these cases, we can study the effect of small particles on the structure of large particles by considering an effective potential for a one component SHS system for which the phase behavior of this one-component system is the same as the phase behavior of the large particles in our two component systems.

3.1. Spinodal phase transition

The spinodal transitions are important to the solution stability and physical mechanisms of colloidal gelation. It has been shown that for a bridging attraction system, the gelation is still driven by the frustrated arrested spinodal decomposition transition, when the volume fraction is less than

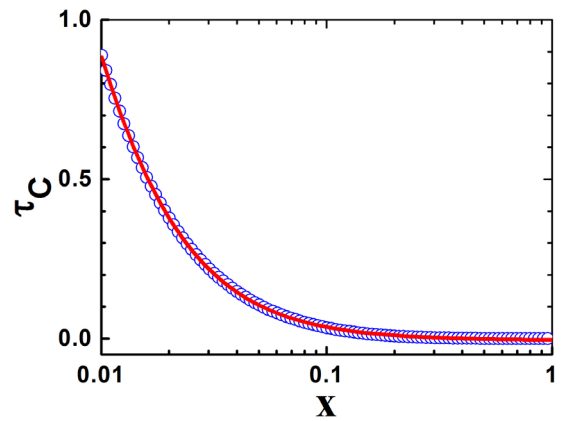


Figure 2. The critical stickiness parameter for different size ratio (blue open circles), where the red solid line is the fit to an empirical function. The horizontal axis is in logarithmic scale.

10% [27]. This is similar to depletion attraction systems [39]. The spinodal decomposition regions of large particles in our two-component systems can be identified by calculating the inter-particle structure factor, $S_{LL}(Q)$, for large colloidal particles. By allowing $1/S_{LL}(0)$ to approach zero, we can identify the spinodal phase separation boundaries [37]. The spinodal decomposition line (SDL) for systems with a bridging attraction can be calculated using the following equation within the framework of two-component SHS model as [28, 37, 40]

$$\begin{aligned}
 & 3 + \sqrt{\left(3 + \frac{1-\phi}{\phi_S}\right)\left(3 + \frac{1-\phi}{\phi_L}\right)} \\
 & \frac{\frac{(1+x)^2}{4x}(1-\phi)}{(1+x)(1-\phi) + 3(\phi_S + x\phi_L)} \\
 & = \frac{\frac{1-\phi}{4x}(\phi_S + x\phi_L)(1+x)^2 + (1+x)(1-\phi)^2\tau}{} \tag{2}
 \end{aligned}$$

where ϕ_S, ϕ_L are the volume fractions of small and large colloidal particles, respectively, and $\phi = \phi_S + \phi_L$ is the total volume fraction.

The effects of x and τ on the SDLs are summarized in figures 1(A) and (B). The volume fraction of large particles and small particles are chosen to be the horizontal and vertical axis, respectively, to be consistent with the previous experimental and theoretical results [25–28]. The volume fraction of large particles is truncated below 40%, near which the demixing spinodals between uniform phases could be preempted by a fluid–solid transition/demixing. Before adding small particles, large colloidal particles are stable in solution. Adding small particles increases the effective attraction between large colloidal particles [28]. And once reaching a maximum attraction strength, adding even more small particles decreases the effective attraction strength. Hence, adding a small amount of small particles favors the formation of aggregates. When ϕ_L is larger than a certain threshold value, the system can enter the spinodal region immediately. If more small particles are added, the effective attraction between the large particles becomes weak enough that the system can exit the spinodal region. Hence, the spinodal region in these systems can form an isolated island.

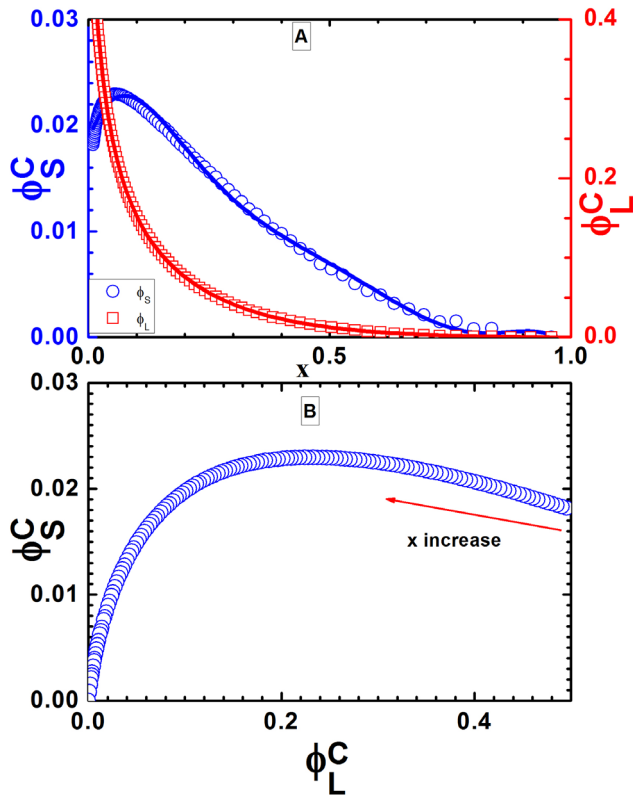


Figure 3. (A) The critical volume fraction of small particles (blue open circles, left vertical axis) and large particles (red open squares, right vertical axis) for the critical point with increasing size ratio. The solid lines are their fitting results with expressions in the text. (B) The trace of critical point when increasing size ratio (arrow direction).

As shown in figure 1(A), increasing τ (decreasing the attraction strength) at a given size ratio ($x = 0.05$ in this case) shrinks the area of the spinodal island while the center of the island remains at almost the same position. When τ is large enough to reach a critical value, τ_C , the isolated spinodal region shrinks to a singular point. For τ larger than τ_C , there is no spinodal region any more based on our theoretical calculations. For these cases, the system remains in a liquid state without gas-liquid phase separation as a function of ϕ_S and ϕ_L . The size effect on the SDLs is summarized in figure 1(B). For a given τ value, increasing the size ratio also shrinks the spinodal island. However, the center of the spinodal island moves to a much smaller total volume fraction.

τ_C is determined solely by the size ratio. By knowing the value of τ_C , we then know the minimum attraction strength needed to destabilize a solution. Figure 2 shows τ_C as a function of the size ratio, x , with a logarithmic scale of the horizontal axis to show more details in the small size ratio range. For a given size ratio, if the attraction between the small and large particle is weak enough that τ is larger than τ_C , no phase separation will be observed in this system. τ_C simply decreases when increasing the size ratio. Physically, it means that when decreasing the size difference (increasing the size ratio, x), a stronger attraction (smaller stickiness parameter) between small and large components is required to introduce a phase separation. When the size ratio reaches $x = 1$, τ_C is almost

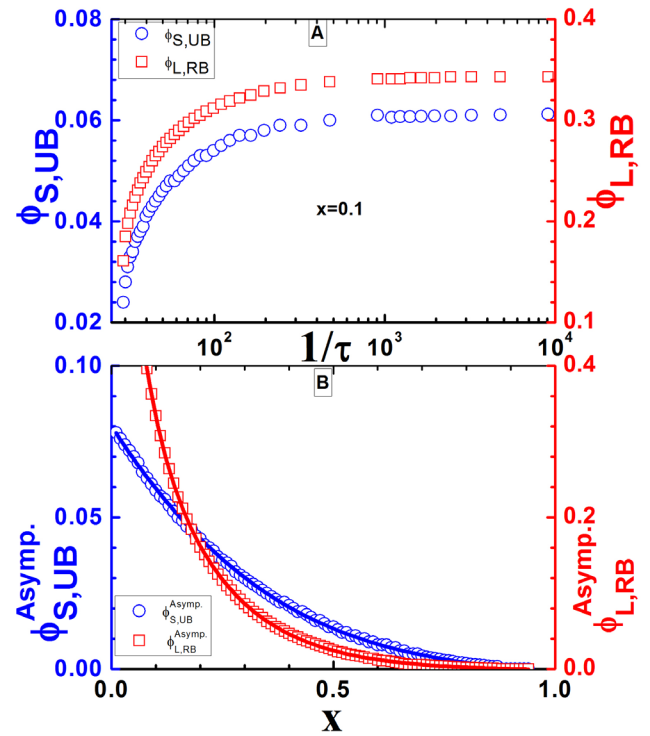


Figure 4. (A) The upper boundary (maximal volume fraction of the small component, blue open circles, left vertical axis) and right boundary (maximal volume fraction of the large component, red open squares, right vertical axis) of the spinodal island for fixed size ratio $x = 0.1$, changing with inverse stickiness parameter. The horizontal axis is logarithmic scale. (B) The maximum spinodal island for different size ratios. These are the asymptotic values from (A). The symbols are the same, and the solid lines are the empirical fits.

zero (corresponding to infinitely strong attraction), which means the system will never show phase separation within the framework of the current theory.

The relationship of the critical stickiness parameter with the size ratio can be fitted to an empirical function as

$$\tau_C = -5.390 \times 10^{-3} + \frac{4.030}{1 + [x/(4.160 \times 10^{-3})]^{1.433}} \quad (3)$$

This type of functional form has been commonly used in pharmacology and chemistry. Equation (3) can help experimentalists decide the attraction strength needed to introduce or prevent the systems' phase separation according to the size of the colloidal and additive small particles.

At $\tau = \tau_C$, the spinodal region reduces to one single point in the phase diagram as well as the binodal region. The concentrations for small and large particles for this singular point are denoted as ϕ_S^C and ϕ_L^C . Figure 3(A) shows the values of ϕ_S^C (blue open circles) and ϕ_L^C (red open squares) as a function of the size ratio, x . Note that the vertical axes on the left and right indicate the values for ϕ_S^C and ϕ_L^C , respectively. ϕ_L^C decreases monotonically to zero with increasing size ratio, while ϕ_S^C has a small increase at very small size ratio and then also gradually decreases to zero when the size ratio approaches 1. Figure 3(B) shows how the singular phase separation point moves in the (ϕ_L, ϕ_S) plane. The arrow

in the figure indicates the direction of its movement when increasing the size ratio. ϕ_L^C for large particles can be fitted by an empirical function as

$$\phi_L^C = 0.246 \times \exp\left(-\frac{x}{0.04}\right) + 0.223 \times \exp\left(-\frac{x}{0.01}\right) + 0.235 \times \exp\left(-\frac{x}{0.176}\right) - 1.17 \times 10^{-3}. \quad (4)$$

And for ϕ_S^C , it can be fitted by a 6th-order polynomial as:

$$\phi_S^C = 1.846 \times 10^{-2} + 0.136x - 1.337 \times x^2 + 4.478 \times x^3 - 7.390 \times x^4 + 5.954 \times x^5 - 1.860 \times x^6. \quad (5)$$

Both fitting lines are shown in figure 3(A).

Based on the results of figure 1, we see that decreasing τ or decreasing the size ratio, x , make the spinodal island bigger. To characterize the change of the spinodal island, we study the change of the upper boundaries of the spinodal decomposition region as a function of the size ratio, x . The upper boundary values of the small and large particle's volume fractions for the spinodal region are denoted as $\phi_{S,UB}$ and $\phi_{L,RB}$. Figure 4(A) shows how $\phi_{S,UB}$ and $\phi_{L,RB}$ change as a function of the inverse stickiness parameter for a fixed size ratio of $x = 0.1$. The left vertical axis is the upper boundary for $\phi_{S,UB}$, which is the maximal volume fraction of the small component and is represented by blue open circles. The right vertical axis is the upper boundary of $\phi_{L,RB}$, which is the maximal volume fraction of the large particles, and is represented by red open squares. The horizontal axis is a logarithmic scale to include a large enough range to show the asymptotic properties. When increasing the inverse stickiness parameter (increasing the attraction strength between small and large particles), both $\phi_{S,UB}$ and $\phi_{L,RB}$ increase very quickly at the beginning, and then reach a plateau value when the attraction strength is very large. The increase of $\phi_{S,UB}$ and $\phi_{L,RB}$ is associated with the increase of the spinodal decomposition region. Hence, the area of the spinodal island increases first and then reaches a saturation value. Increasing the attraction strength further results in little additional motion of the phase boundary.

We can define the asymptotic value of $\phi_{S,UB}$ and $\phi_{L,RB}$ at large attraction strength as the values at which the area of the spinodal decomposition island changes less than 1% when the stickiness parameter changes 10%. Since they are the asymptotic values of $\phi_{S,UB}$ and $\phi_{L,RB}$, a superscript 'Asymp.' is used to describe the value. These asymptotic values show the largest possible spinodal region when increasing the attraction strength at a fixed value of x . Their changes with the size ratio, x , are shown in figure 4(B). The symbols are the same with figure 4(A) and the solid lines are the empirical fitting results. Both $\phi_{S,UB}^{Asymp.}$ and $\phi_{L,RB}^{Asymp.}$ simply decrease with the increasing size ratio, meaning when the size ratio is large (the size of two types of particles become closer to each other), it becomes more difficult to separate the system phase. When the size ratio approaches 1, the spinodal region disappears. $\phi_{S,UB}^{Asymp.}$ can be fitted by a 3rd-order polynomial as

$$\phi_{S,UB}^{Asymp.} = 0.080 - 0.228x + 0.234x^2 - 0.088x^3. \quad (6)$$

And $\phi_{L,RB}^{Asymp.}$ can be fitted by a two-decay factor exponential function as

$$\phi_{L,RB}^{Asymp.} = 0.533 \times \exp\left(-\frac{x}{0.167}\right) + 0.449 \times \exp\left(-\frac{x}{0.042}\right) - 2.120 \times 10^{-3}. \quad (7)$$

These two equations quantitatively explain how large the spinodal island could be for a given fixed size ratio if the attraction strength is strong enough. If the volume fraction of small or large colloidal particles is larger than its asymptotic value, the system will be out of the spinodal region no matter how strong the attraction is.

We have tried to obtain analytical solutions for theoretical results shown above (equations (3)–(7)) since the spinodal transition boundary has an analytical expression (equation (2)). To do this, we need to express ϕ_S as a function of ϕ_L , which is the solution of a 4th-order polynomial function with ϕ_S and ϕ_L coupled with each other. It is very difficult to obtain the analytical solution by solving this equation. To simplify the effort for readers to use our results, the empirical functions are used with enough precision to help guide the design of future experimental systems.

When calculating the spinodal transition boundaries, the theory can accommodate any particle size ratio. In the following two sections, we will focus on the cases where x is small enough that small particles can be treated as solvent molecules.

3.2. Pair distribution function and effective inter-particle potential

The partial structure factor (PSF) is the Fourier transform of the pair distribution function (PDF) as [41]:

$$S_{ij}(q) = \delta_{ij} + (n_i n_j)^{1/2} \int d^3r e^{i\vec{q} \cdot \vec{r}} (g_{ij}(r) - 1) \quad (8)$$

where $S_{ij}(q)$ is the PSF between component i and j , $g_{ij}(r)$ is their PDF, and n_i is the number density of component i and δ_{ij} is Kronecker delta function. This theory provides the method to calculate the PDF from PSF through an inverse Fourier transform while the PDF can be calculated using the multi-component SHS framework [28, 34]. In a relatively dilute system, the PDF can be simply related to the effective pairwise potential $U(r)$ between large particles as [42]:

$$g(r) = e^{-\beta U(r)}. \quad (9)$$

We thus can estimate the effective interaction potential between large colloidal particles by calculating its PDF similar to that studied by a recent work [40]. Figure 5(A) shows the PDFs of large colloidal particles as a function of small particle volume fraction with fixed parameters $\phi_L = 0.001$, $\tau = 0.1$, $x = 0.01$. The horizontal axis is the inter-particle distance between large particles normalized by d_L . Since the colloids are hard spheres, they cannot overlap in space and $g(r)$ is zero when the distance is smaller than its

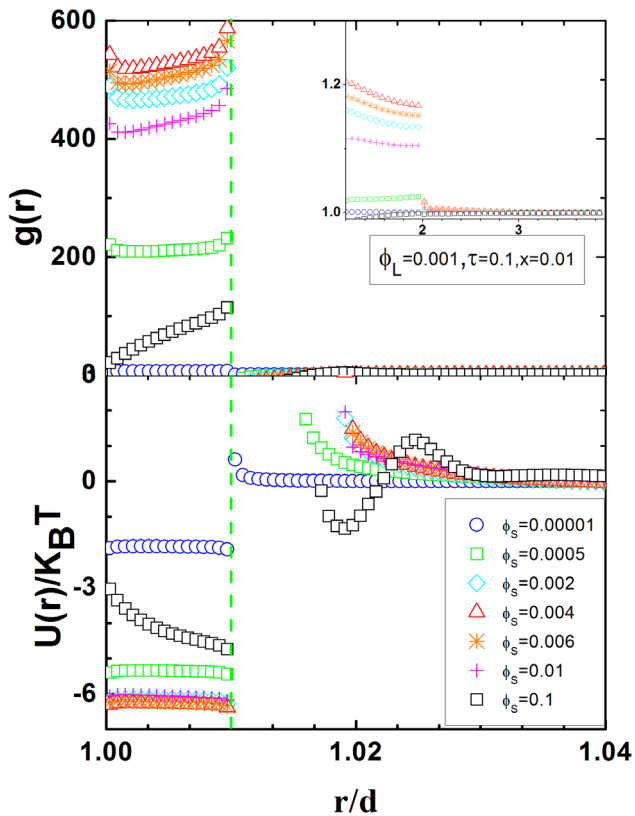


Figure 5. (A) Pair distribution function of colloidal particles for systems with $\phi_L = 0.001$, $\tau = 0.1$, $x = 0.01$ and different volume fractions of the small component, the horizontal axis is the interparticle distance normalized to d_L . The results are plotted in a limited range to show the details of properties in a small range of interaction distance, while the inset shows overall results. (B) The effective pair potential for the same systems are shown for the cases presented in (A). The vertical green dashed line is drawn at $r/d = 1 + d_s/d_L$.

diameter. With the addition of small particles, a plateau with a value larger than one shows up in the range defined by the diameter of small particles, indicating a large probability for the connection of two large colloidal particles through a small particle. This increased intensity is due to the formation of clusters introduced by the bridging attraction.

When the concentration of small particles increases at the beginning, the probability of connection increases dramatically as shown by the increased $g(r)$ at $r/d \approx 1$. For the current example, this increasing trend continues until the volume fraction of small particles reaches $\phi_s = 0.004$ (red open triangles), up to the point where the effective pair attraction reaches a maximum that has been designated as the maximum bridging attraction point [28]. Further increasing the small particle concentration decreases the effective attraction.

Using equation (9), the effective potential between large particles can be evaluated using $g(r)$. The results are shown in figure 5(B). Clearly, due to the existence of small particles, there is a primary attraction close to the large particle surface, with an attractive range exactly the size of small particles as depicted by the vertical green dashed line. Hence, the interaction range for the bridging attraction is

determined by the size of the small particles. The strength of this effective attraction is a function of the small particle concentration. It first increases to a maximum at $\phi_s = 0.004$ and then decreases, following the decrease in $g(r)$. Besides the strong short-range attraction, there are oscillations for $r/d > 1 + x$. This is due to the packing of the small particles on the large particle surface, which introduces an effective repulsive potential.

Our previous work [28] showed that the effective potential between the large particles in this two component SHS system can be mapped to an effective one-component SHS interaction, as long as we are only concerned with the phase behavior of the large particles. This immediately implies that the detailed oscillations of the effective interaction between large particles are not important in the two component systems. As long as the calculated normalized B_2^* is the same, the equilibrium phase diagram of the colloidal particles is the same, so long as their interactions are all short ranged. This conclusion is very interesting. Noro and Frankel have studied different types of purely attractive potentials with different ranges and shapes, and pointed out that the equilibrium phase diagram close to the critical point is not sensitive to the ranges and shapes of the short-range attraction [35]. The reduced second virial coefficient, B_2^* , uniquely determines the phase diagram of a system with a short-ranged potential. Our results here together with our previous work [28] show that the extended law of the equation of state works not only for many different types of purely attractive potentials, but also for the short-range interaction systems even when they have complicated small repulsive features in the effective interaction potential as indicated in our case. As long as the calculated B_2^* is overall attractive and the overall interaction range is short ranged, the equilibrium phase diagram still follows the extended law of the equation of state proposed originally by Noro and Frankel [35].

3.3. Percolation and binodal region

Previously, we proposed a method to understand the phase behavior of a binary SHS system by an equivalent one-component SHS system where the structures and the phase behavior of the large colloidal particles in the binary system are identical to those from an equivalent one-component system [28] as long as the small particles in this binary system are small enough. For a given conditions of the two-component systems, we need to determine three parameters, τ^{eff} , d_L^{eff} , and ϕ_L^{eff} , for the equivalent one-component SHS system. Once the three parameters are determined with the method, many results for pure one-component SHS systems, including the calculations of percolation and binodal transitions, can be applied to systems with the bridging attraction [28]. We briefly present the final results of this method here about how to determine these three parameters. The details were given in our previous work [28].

The equivalent stickiness parameter is calculated by equating the PSF of the large colloidal particles $S_{LL}(q)$ at $q = 0$, and is expressed as [28]:

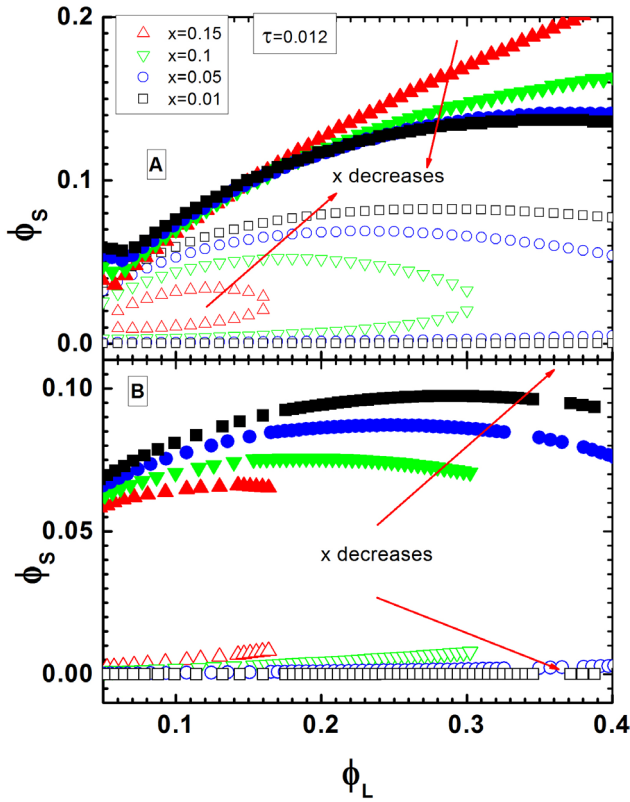


Figure 6. (A) Upper percolation transition line (filled symbols) when decreasing size ratio (arrow direction), along with spinodal islands (open symbols) in the volume fraction plane. (B) Binodal transition regions change with decreasing size ratio (arrow direction), the lower boundary is in open symbols and the upper boundary in filled symbols. The stickiness parameter is fixed to be $\tau = 0.012$ and the corresponding size ratios can be found in the legend of (A). A combination of the upper boundaries of percolation and binodal transition can be found in the supporting information.

$$\tau_L^{\text{eff}} = \left[\frac{(1 - \phi_L^{\text{eff}})^2}{36} \frac{1}{S_{LL}(0)} + \frac{4\phi_L^{\text{eff}} - 1}{18} \frac{1}{\sqrt{S_{LL}(0)}} - \frac{14(\phi_L^{\text{eff}})^2 - 4\phi_L^{\text{eff}} - 1}{36(1 - \phi_L^{\text{eff}})^2} \right] / \left[\frac{2\phi_L^{\text{eff}} + 1}{3(1 - \phi_L^{\text{eff}})} - \frac{1 - \phi_L^{\text{eff}}}{3} \frac{1}{\sqrt{S_{LL}(0)}} \right]. \quad (10)$$

The effective diameter, d_L^{eff} , is simply related to the size ratio by the following equation [28]:

$$\frac{d_L^{\text{eff}}}{d_L} = \frac{2}{3} \left(1 + x + \frac{1}{2 + x} \right) \quad (11)$$

And the effective volume fraction, ϕ_L^{eff} , is given by [28]:

$$\frac{\phi_L^{\text{eff}}}{\phi_L} = \left(\frac{d_L^{\text{eff}}}{d_L} \right)^3 \quad (12)$$

This method works effectively when $x < 0.15$ and $\tau < 2$ (please check the supplementary information for more details (stacks.iop.org/JPhysCM/28/455102/mmedia)). With equations (10)–(12), the binodal transition and percolation of large

particles in our two-component system can be calculated by comparing to the literature results of one component SHS system.

The percolation line of the pure one-component SHS system is calculated analytically by Chiew and Glandt with the PY approximation as [43]:

$$\tau_L^{\text{eff}} = \frac{19\phi_L^{\text{eff}2} - 2\phi_L^{\text{eff}} + 1}{12(1 - \phi_L^{\text{eff}})^2}. \quad (13)$$

The binodal transition line has been calculated by Miller and Frenkel through the grand canonical MC simulation [44]. Based on these results, we have estimated the size effects on the percolation and binodal transitions, which are shown in figures 6(A) and (B), respectively. Here, the stickiness parameter is fixed at $\tau = 0.012$, which is the value we previously used to calculate the theoretical phase diagram of Zhao's experimental system [28].

Figure 6(A) shows the upper percolation transition lines (filled symbols) together with the spinodal lines (open symbols) when decreasing the size ratio from 0.15 to 0.01 (arrow indicates the direction of decreasing the size ratio). When ϕ_L is large enough, adding small particles introduces a bridging attraction to form percolated clusters in solution. When adding too many small particles, the attraction becomes weak and the system enters a non-percolated liquid region. Therefore, similar to the spinodal transitions, there are two percolation transition volume fractions for small particles at a given ϕ_L . We term them as the lower percolation transition line and the upper percolation transition line. The lower percolation transition line, in general, has very small values (smaller than that of spinodal decomposition lines shown in the same figure), and is very sensitive to small changes of small particle volume fraction, ϕ_S , and is not shown in the figure. Usually, it is challenging to control the sample behavior near the lower percolation transition boundary. On the other hand, the effective bridging attraction changes near the upper percolation transition line is not so sensitive to ϕ_S . Hence, it is easier to control the effective potential close to the upper percolation transition line, so we focus on discussing the size effects on this transition line.

It is noted that for $\phi_L < 0.2$, the upper percolation transition line is not very sensitive to the change of the size ratio. For $\phi_L > 0.2$, increasing size ratio shifts down the upper percolation transition line. For $\phi_L < 0.1$, the upper percolation transition line is very close to the spinodal decomposition region, which is consistent with a recent experimental result [27].

Figure 6(B) shows the binodal lines when changing the size ratio. The binodal line is expected to form an isolated island similar to the spinodal island. However, since the system is close to the instability line, the calculated structure factor from Baxter's method for a one component system is not very accurate at small ϕ [28, 29]. Hence, data smaller than $\phi_L = 0.05$ are not reported. At large volume fractions, we are limited by the available values from the computer simulations to determine the binodal line in a one-component SHS system [44]. Differing from the percolation region, the binodal transition region expands when decreasing the size ratio. This is

consistent with the change of the spinodal decomposition region.

We have also studied the attraction strength effect at a given fixed size ratio on the percolation transitions and binodal transitions. (Please see the supporting information for details.) Increasing attraction strength expands the percolation region by shifting up the upper percolation transition line and shifting down the lower percolation transition line. However, it seems that there are larger shifts at smaller volume fractions rather than at larger volume fractions. This differs from what is observed for the change of the size ratio, where the large shift for the change of size ratio mainly happens at large ϕ_L . As for the binodal regions, they also expand when increasing the attraction strength with the center position of the binodal region staying in almost the same position. This is consistent with what is observed for the change of the spinodal islands due to the variation of the attraction strength.

The fluid-solid transition is more difficult to predict. It is well known that for a hard sphere system, the liquid-solid transition occurs when the height of the first peak of the static structure factor reaches about 2.85 [45]. This is called Hansen–Verlet criterion. However, for a system with a depletion attraction, the Hansen–Verlet criterion is found to work only for large volume fraction of big particles. [19, 46] Even though it is not clear how it may work in a bridging attraction system, we have calculated the boundary lines at which the peak height of the static structure factor is 2.85. The details are shown in the supporting information.

4. Conclusion

Adding small particles to a system is a common method to tune the inter-particle interaction of colloidal particles and control the phase behavior of large colloidal particles. Colloidal systems based on both depletion attraction and bridging attraction can be considered as binary systems. In the depletion attraction case, small particles are not attracted to the surface of large particles while for the bridging attraction systems, small particles can be strongly, but reversibly, attracted to the surface of large particles. Hence, the depletion attraction and bridging attraction are two extreme cases of binary hard sphere systems. Compared to the well-studied depletion attraction system, there are very few studies on bridging attraction systems. Here, we successfully apply Baxter’s multi-component theory and previously proposed methods to study the phase behavior of bridging attraction systems with a focus on the size effects on the spinodal transition, effective interaction, binodal transition and percolation transition.

When decreasing the attraction strength (increasing τ), the spinodal island shrinks. And it eventually shrink to a singular point when $\tau = \tau_c$. Hence, there is a minimum attraction strength that is needed to introduce a phase separation. For $\tau > \tau_c$, the systems are stable. τ_c is a function of the size ratio, x , and its dependence on x is estimated and fitted with an empirical formula. Knowing this value of τ_c is critical to tune the stability of a binary SHS system. Future experimental work is necessary to check the accuracy of our theoretical results. The volume fractions for the small and large particles

for this singular point are also studied as a function of the size ratio.

For a fixed size ratio, the spinodal decomposition island expands its area when the attraction strength is increased. When the attraction strength is large enough, the spinodal island reaches a saturation boundary. The asymptotic value of the spinodal island at infinitely strong attraction strength is very sensitive to the size ratio between small and large particles.

The pair distribution function of colloidal particles, $g(r)$, is also calculated for different small particle concentrations, from which the effective pair potential is estimated at small concentrations of large particles. The main feature of the effective pair potential is a square well hard sphere interaction, where its range is the size of the small particles. Its attraction strength is determined by the volume fraction of small particles. When increasing the small particle concentration, repulsive barrier in a certain range of the interaction distance can appear in the effective potential even though the overall interaction is still attractive. However, despite the complex details of the effective potential obtained from the binary systems with the bridging attraction, the structure factor of large colloidal systems can be always approximated by an equivalent one-component system where the inter-particle potential can be simplified to Baxter’s SHS potential. This immediately implies that the Noro–Frankel’s extended law of the equation of state is not only valid for purely attractive potentials, but also for more complex potentials including repulsive features as long as the overall interaction is still short-ranged and B_2^* is still dominated by the attractive potential.

The percolation and binodal transitions are studied for our binary systems by using a mapping method proposed previously, which works quite well when $x < 0.15$ and $\tau < 2$. The percolation region shrinks with size ratio decreasing. The binodal transition region expands when the size ratio decreases.

There are many systems that can be approximated by a bridging attraction model, such as oppositely charged colloidal particles and proteins with counterions of large valency. Our results here can aid the design of new colloidal systems with desired stability or instability, and support the understanding of complex phenomena in concentrated protein solutions.

Acknowledgments

This manuscript was prepared under the partial support of the cooperative agreement 70NANB10H256 from NIST, U.S. Department of Commerce. The statements, findings, conclusions and recommendations are those of the authors and do not necessarily reflect the view of NIST or the U.S. Department of Commerce.

References

- [1] Chen S H, Liao C, Fratini E, Baglioni P and Mallamace F 2001 *Colloids Surf. A* **185** 95
- [2] Yearley E J *et al* 2014 *Biophys. J.* **106** 1763
- [3] Velev O D, Kaler E W and Lenhoff A M 1998 *Biophys. J.* **75** 2682

- [4] Doster W and Longeville S 2007 *Biophys. J.* **93** 1360
- [5] Godfrin P D, Hudson S D, Porcar L, Falus P, Wagner N J and Liu Y 2015 *Phys. Rev. Lett.* **115** 228302
- [6] Poon W C K 2004 *MRS Bull.* **29** 96
- [7] Pusey P N, Pirie A D and Poon W C K 1993 *Physica A* **201** 322
- [8] Ilett S M, Orrock A, Poon W C K and Pusey P N 1995 *Phys. Rev. E* **51** 1344
- [9] Fernandes G E, Beltran-Villegas D J and Bevan M A 2008 *Langmuir* **24** 10776
- [10] Fernandes G E, Beltran-Villegas D J and Bevan M A 2009 *J. Chem. Phys.* **131** 134705
- [11] Xing X, Li Z and Ngai T 2009 *Macromolecules* **42** 7271
- [12] Meng G, Arkus N, Brenner M P and Manoharan V N 2010 *Science* **327** 560
- [13] Bayliss K, van Duijneveldt J S, Faers M A and Vermeer A W P 2011 *Soft Matter* **7** 10345
- [14] Anderson V J and Lekkerkerker H N W 2002 *Nature* **416** 811
- [15] Oosawa F and Asakura S 1954 *J. Chem. Phys.* **22** 1255
- [16] Evans R and Napper D H 1973 *Nature* **246** 34
- [17] Lekkerkerker H N W and Stroobants A 1993 *Physica A* **195** 387
- [18] Gotzelmann B, Evans R and Dietrich S 1998 *Phys. Rev. E* **57** 6785
- [19] Dijkstra M, van Roij R and Evans R 1999 *Phys. Rev. E* **59** 5744
- [20] Dijkstra M, van Roij R and Evans R 1998 *Phys. Rev. Lett.* **81** 2268
- [21] Leunissen M E, Christova C G, Hynninen A P, Royall C P, Campbell A I, Imhof A, Dijkstra M, van Roij R and van Blaaderen A 2005 *Nature* **437** 235
- [22] Guerrero-Garcia G I, Gonzalez-Tovar E and de la Cruz M O 2010 *Soft Matter* **6** 2056
- [23] Zhang F et al 2008 *Phys. Rev. Lett.* **101** 148101
- [24] Roosen-Runge F, Zhang F, Schreiber F and Roth R 2014 *Sci. Rep.* **4** 7016
- [25] Zhao C, Yuan G and Han C C 2012 *Macromolecules* **45** 9468
- [26] Zhao C, Yuan G and Han C C 2012 *Soft Matter* **8** 7036
- [27] Luo J, Yuan G, Zhao C, Han C C, Chen J and Liu Y 2014 *Soft Matter* **11** 2494
- [28] Chen J, Kline S R and Liu Y 2015 *J. Chem. Phys.* **142** 084904
- [29] Baxter R J 1968 *J. Chem. Phys.* **49** 2770
- [30] Baxter R J 1968 *Aust. J. Phys.* **21** 563
- [31] Goldfrin P D, Zarraga I E, Zarzar J, Porcar L, Falus P, Wagner N J and Liu Y 2016 *J. Phys. Chem. B* **120** 278
- [32] Piazza R 2004 *Curr. Opin. Colloid Interface Sci.* **8** 515
- [33] Watts R O, Henderson D and Baxter R J 1971 *Advances in Chemical Physics: Chemical Dynamics: Papers in Honor of Henry Eyring* vol 21, ed J O Hirschfelder and D Henderson (Hoboken, NJ: Wiley)
- [34] Baxter R J 1970 *J. Chem. Phys.* **52** 4559
- [35] Noro M G and Frenkel D 2000 *J. Chem. Phys.* **113** 2941
- [36] Barboy B 1974 *J. Chem. Phys.* **61** 3194
- [37] Barboy B 1975 *Chem. Phys.* **11** 357
- [38] Perram J W and Smith E R 1975 *Chem. Phys. Lett.* **35** 138
- [39] Lu P J, Zaccarelli E, Ciulla F, Schofield A B, Sciortino F and Weitz D A 2008 *Nature* **453** 499
- [40] Fantoni R, Giacometti A and Santos A 2015 *J. Chem. Phys.* **142** 224905
- [41] Nagele G 1996 *Phys. Rep.* **272** 215
- [42] Nagele G 2004 *The Physics of Colloidal Soft Matter* (Warsaw: Centre of Excellence for Advanced Materials and Structures)
- [43] Chiew Y C and Glandt E D 1983 *J. Phys. A: Math. Gen.* **16** 2068
- [44] Miller M A and Frenkel D 2004 *J. Chem. Phys.* **121** 535
- [45] Hansen J P and Verlet L 1969 *Phys. Rev.* **184** 151
- [46] Dijkstra M, Brader J M and Evans R 1999 *J. Phys.: Condens. Matter* **11** 10079